Double Optical Gating of High-Order Harmonic Generation with Carrier-Envelope Phase Stabilized Lasers

Hiroki Mashiko, Steve Gilbertson, Chengquan Li, Sabih D. Khan, Mahendra M. Shakya, Eric Moon, and Zenghu Chang[*]

J. R. Macdonald Laboratory, Department of Physics, Kansas State University, Manhattan, Kansas 66506, USA
(Received 29 August 2007; published 14 March 2008)

We demonstrated a novel optical switch to control the high-order harmonic generation process so that single attosecond pulses can be generated with multiple-cycle pulses. The technique combines two powerful optical gating methods: polarization gating and two-color gating. An extreme ultraviolet supercontinuum supporting 130 as was generated with neon gas using 9 fs laser pulses. We discovered a unique dependence of the harmonic spectra on the carrier-envelope phase of the laser fields, which repeats every 2π radians.

Single isolated attosecond pulses are powerful tools for studying electron dynamics in atoms [1]. Such pulses, as short as 130 as, have been generated by the polarization gating (PG) technique [2]. The duration of the laser pulses that form the PG pulses is 5 fs, corresponding to two optical cycles. Although high power 5 fs lasers centered at $\sim$750 nm have been developed for many years [3], it is still a technical challenge to reproduce daily such pulses. Since the first demonstration of generating such attosecond pulses in 2001 [4], very few laboratories have access to such unique light sources.

Experimentally, the PG pulses have been generated by combining two counter-rotating circularly polarized laser pulses with a proper delay [5–9]. The depletion of the ground state population of the atom by the leading edge of the laser pulse sets the upper limit on the driving pulse's duration [10]. In this Letter, we suggest adding a weak second harmonic field to the PG field in order to reduce the depletion so that single attosecond pulses can be generated with multiple-cycle laser pulses. This approach is dubbed double optical gating (DOG).

The laser field with a time-dependent ellipticity for PG can be resolved into a driving field and a gating field. Figure 1 shows the driving field components for (a) PG and (b) DOG. When the amplitude of the second harmonic field is high enough, the spacing between adjacent attosecond pulses becomes one full optical cycle, as depicted in Fig. 1(b) as compared to the half-cycle spacing in PG as in Fig. 1(a) [11–13]. As a result, for double optical gating, the width of the polarization gate can be close to 1 fundamental wave cycle to allow the emission of a single attosecond pulse, which is a factor of 2 larger than what is required by conventional PG. These gate widths were used in Fig. 1(c) to show the ionization probability of an argon atom in the PG and DOG fields as a function of the input pulse duration. The intensity is 2.8×10^{14} W/cm^2. The ADK ionization rate was used for the calculation [14]. Obviously the wide gate corresponding to DOG signifi-

cantly reduces the depletion of the ground state population. As a result, the longest pulses one can use for generating single attosecond pulses with DOG are 12 fs, which is almost a factor of 2 larger than those applicable to the conventional PG ($\sim$6.5 fs).

The DOG was demonstrated with a carrier-envelope phase stabilized chirped pulse amplifier (CPA) followed by a hollow-core fiber compressor [15,16]. The CPA laser produces 25 fs, 2.5 mJ pulses centered at 790 nm at 1 kHz. The CE phase stabilization of the oscillator was accomplished by the self-referencing technique [17,18]. The slow drift from the amplifier was compensated by feedback control of the grating separation [19,20]. The output beam from the hollow-core fiber and chirped mirrors was incident onto a nonlinear crystal for the second harmonic generation. We used a barium borate (BBO) crystal with a thickness of 250 μm.

The double gating laser field was synthesized in a Mach-Zehnder interferometer. The second harmonic and fundamental beams were separated by a dichroic beam splitter. The fundamental arm was equipped with a PZT delay stage to control the relative delay between the two arms. The same PZT was also used to stabilize the relative delay by using a cw laser beam propagating inside the interferometer as feedback. The PG pulse was produced by a birefringent quartz plate (0.4 mm) and an achromatic quarter-wave plate (2 mm). These conditions yielded a calculated polarization gate width of $\sim$2 fs. The SH and the PG field were combined by another beam splitter. After the interferometer, we measured the pulse duration of the fundamental pulse using the frequency resolved optical gating to be 9.1 fs and nearly transform limited.

The DOG laser beams were focused by a spherical mirror ($f = 400$ mm) to a gas filled interaction cell with pressure of 10 torr and length 1.4 mm. The gas target was placed approximately 1.5 mm behind the laser focus but within the Rayleigh ranges of 3.5 mm for the fundamental pulse and 1.75 mm for the second harmonic pulse. In front
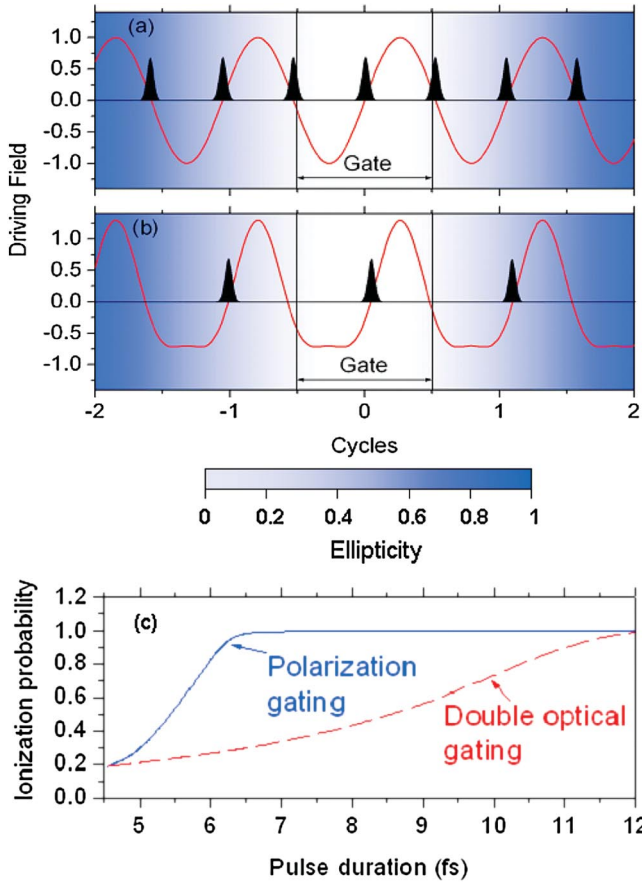
FIG. 1 (color). The driving filed components for PG correspond to (a) without and (b) with the second harmonic field, respectively. The driving field is shown as the red line. The two vertical lines represent the gate width. Here, the filled curves are the attosecond pulses emitted when the driving fields alone are applied. The background color shows the strength of the PG. In figure (c) the ionization probability of an argon atom in the field of PG pulses is compared with that in the field of DOG. The longest pulses that can be used are those at which the probability reaches one.

of the cell, the energies of the fundamental and second harmonic pulses were 150 and 30 μJ, respectively. The estimated effective intensities inside the gate were 2.8×10^{14} W/cm^2 and 7×10^{13} W/cm^2, respectively. The generated harmonics were measured with a grating spectrometer.

The laser field can be expressed as the combination of two perpendicularly polarized fields $\vec{E}(t) = E_{\text{drive}}(t)\hat{i} + E_{\text{gate}}(t)\hat{j}$. The driving field is

$$E_{\text{drive}}(t) = E_0[(e^{-2\ln 2[(t+T_d/2)^2/\tau_\omega^2]}$$
$$+ e^{-2\ln 2[(t-T_d/2)^2/\tau_\omega^2]})\cos(\omega_0 t + \varphi_{\text{CE}})$$
$$+ ae^{-2\ln 2(t^2/\tau_{2\omega}^2)}\cos(2\omega_0 t + 2\varphi_{\text{CE}} + \phi_{\omega,2\omega})] \quad (1)$$

and the gating field is

$$E_{\text{gate}}(t) = E_0(e^{-2\ln 2[(t+T_d/2-T_0/4)^2/\tau_\omega^2]}$$
$$- e^{-2\ln 2[(t-T_d/2-T_0/4)^2/\tau_\omega^2]})\sin(\omega_0 t + \varphi_{\text{CE}}), \quad (2)$$

where E_0 is the amplitude of the circularly polarized fundamental laser field with carrier frequency ω_0 (period T_0), pulse duration τ_ω, and CE phase φ_{CE}. T_d is the time delay between the two circular pulses. The delay, $T_0/4$, between the gating and the driving fields is introduced by the quarter-wave plate. $\phi_{\omega,2\omega}$ is the relative phase between the fundamental and second harmonic pulses. The duration of the SH pulse is $\tau_{2\omega}$. Finally, a represents the strength of the second harmonic field relative to the fundamental field.

Figure 2(a) shows harmonic spectra of argon for one-color (linearly polarized fundamental field only, $T_d = 0$, $a = 0$), two-color (a second harmonic field added to a fundamental field polarized in the same direction, $T_d = 0$), conventional PG ($a = 0$), and DOG fields. Notice that
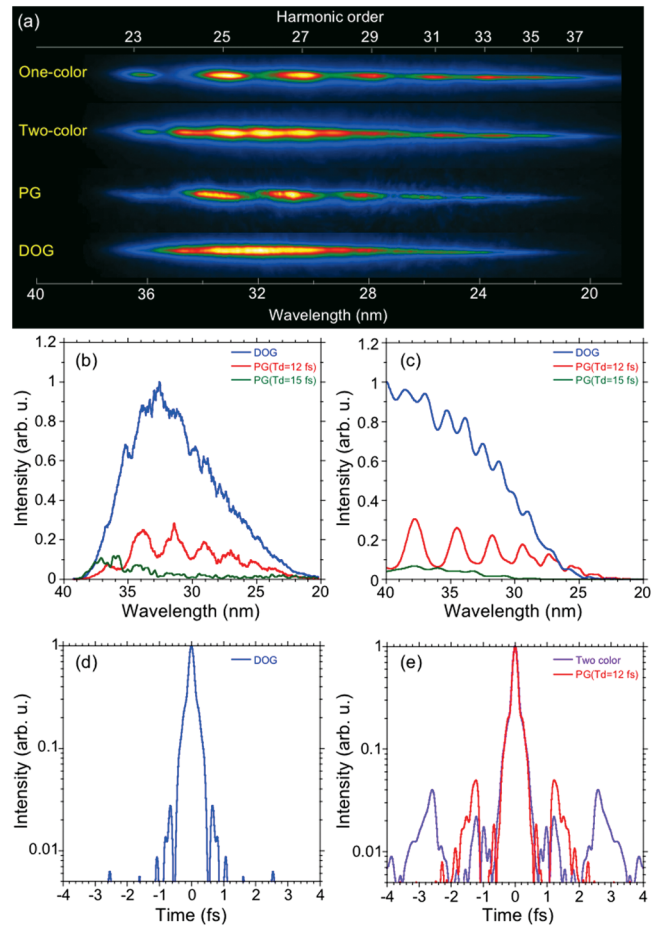

FIG. 2 (color). Comparison of harmonic spectra and pulses. (a) The harmonic spectrum images obtained by various gating methods. The lineout plots in (b) compare the spectral profile and intensity obtained from DOG (blue line) with those from PG for delays of 12 fs (red line) and 15 fs (green line). The results from numerical simulations are shown in (c). (d) Shows the Fourier transform for the DOG and (e) shows the Fourier transforms for the PG and two-color spectra. These were done assuming flat phase.

the spectra on the long wavelength side are clipped by the detector. As expected, only odd order harmonics are generated by the 9 fs one-color field, whereas even harmonics appeared with the two-color laser. The harmonic peaks broadened due to PG, whereas the peaks merged to a supercontinuum as a result of the DOG. Since both the CE phase and the relative phase between the two colors were stabilized, we can rule out the possibility that the supercontinnum was caused by accumulation of many peak-shifted spectra. This is key evidence that the DOG produces a supercontinuum spectrum.

The spectral profiles of the PG spectra with two different delays, T_d, between the two circularly polarized pulses are shown in Fig. 2(b); also shown are the DOG spectra. The red and blue lines are for 12 fs delay while the green line is for $T_d = 15$ fs. The simulated spectra are shown in Fig. 2(c) for comparison. The simulation method is similar to that described in references [9,10], which took into account the phase-matching effects. Although a supercontinuum can be obtained by conventional PG with a 15 fs delay, the spectrum signal for the DOG is 23 times higher indicating much stronger isolated attosecond pulses can be generated. Because of the added SH field, the effective intensity of the linearly polarized part is stronger than conventional gating. This fact, coupled with the reduction in the ground state depletion as mentioned earlier in Fig. 1(c), gives rise to the large enhancement. Figure 2(d) and 2(e) show the temporal components derived from Fourier transforms of the spectra assuming flat phase. The most important concept to note is the reduction of pre or post pulse in the temporal domain with DOG proving that this technique produces isolated single attosecond pulses. The pre or post pulses set the lower limit for the intensity of the probe pulses in many pump-probe attosecond application experiments. When the strength of the satellite pulses is comparable to the probe pulse, the interference between them can produce misleading structures when the signal is plotted versus the time delay, which makes the data analysis difficult.

The dependence of the high harmonic spectrum and intensity on the CE phase of the DOG laser was investigated. The CE phase was varied by controlling the effective grating separation in the laser system [21]. The harmonic spectra are shown in Fig. 3(a) and were measured simultaneously with the CE phase measurement. As the f-$2f$ interferometer that measures our relative CE phase does not give the absolute value of the phase, the results were shifted so that the maximum intensity is located at 0. The intensity of the normalized spectrally integrated signal repeats with a period of 2π, as shown in Fig. 3(b). This is consistent with the predictions from the numerical simulations, also shown for comparison. The multiple small peaks in the measured results are due to laser energy fluctuations. This is different from that of the conventional PG, which has a period of $\varphi = \pi$ [22]. This 2π periodic dependence of the harmonic spectra on the CE phase
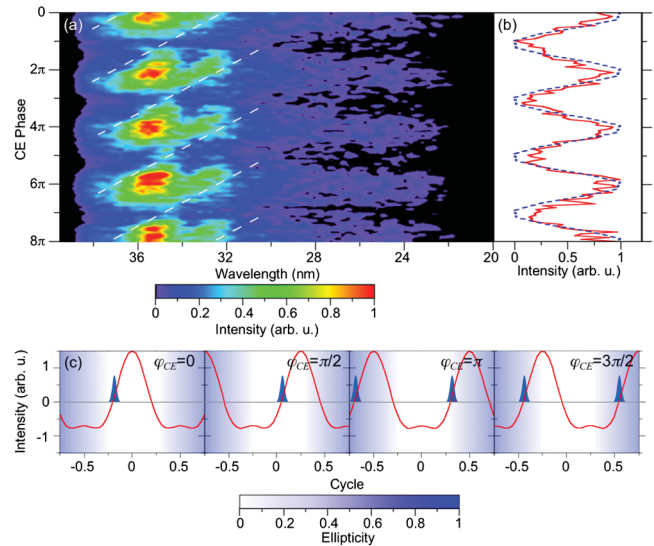

FIG. 3 (color).   The CE phase dependence on the DOG spectra. (a) shows the intensity plot of the harmonic spectrum as the CE phase was scanned through 2π. The normalized integrated signal is shown as the red line in (b). The blue line corresponds to the theoretical predictions. (c) shows the semiclassical predictions of the waveform within the gate width when the CE phase is scanned. The color indicates the strength of the ellipticity.

provides another evidence that the observed supercontinuum is from DOG.

The mechanism of the 2π periodicity can be explained by the three-step model of high harmonic generation [23]. The CE phase φ_{CE} are present in both carrier terms of the driving field in Eq. (1) and the gating field in Eq. (2). The driving field within the polarization gate is depicted in Fig. 3(c). It can be seen that the laser field moves in the gate while the shape of the waveform is unchanged when the CE phase varies. The semiclassic model predicts that the attosecond pulse is emitted near the negative to positive zero crossing in such an asymmetric field. When the crossing is near the center of the gate while the gating power is the weakest ($\varphi_{CE} = 0$ to $\pi/2$), a strong single attosecond pulses is produced. In the spectral domain, it corresponds to an intense supercontinuum. The other emissions are suppressed since they are outside of the gate where the ellipticity is high. For ($\varphi_{CE} = \pi$ to $3\pi/2$), two recollisons are possible. However, they occur near the edges of the gate, and are almost suppressed, which corresponds to a dip in the plot. Since the driving field in the gate repeats when the CE phase changes from 0 to 2π, so does the attosecond emission process. In conventional PG, the symmetry of the laser field and the atoms leads to the same harmonic spectrum for $\varphi_{CE} = 0$ and π, thus the π periodicity.

The split of the continuum into two peaks in Fig. 3(a) represents the evolution from a single electron recollision into two. There is also a spectral peak shift as the CE phase changes, indicated by the slanted dashed lines. This is
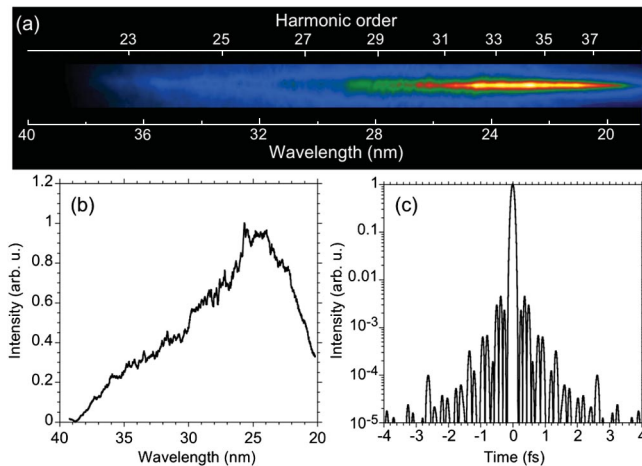
FIG. 4 (color). Results of harmonics generated with a neon target. (a) and (b) show the harmonic spectra and the line profile, respectively. (c) The temporal component derived from the Fourier transform assuming flat phase.

caused by the driving field amplitude variations within the gate width. The phases accumulated by the electrons in the returning trajectories corresponding to the two attosecond emissions are different because of the different fields they experience. The interference pattern in the spectral domain is sensitive to the phase difference just like in the classic Young's two-slit experiments. Since the CE phase determines the number of the electron recollsions and phase of the returning electron wave, it affects the spectral profile. The dramatic variation of the high harmonic spectra as a function of CE phase could lead to yet another method to determine the absolute CE phase with a window of 2π. So far, only π periodicity has been observed in previously reported high harmonic generation studies [2,24]. The well-established phase meter based on measuring above threshold ionization electrons works well for few-cycle pulses, not for ~ 10 fs pulses [25].

Finally, we observed harmonics from neon gas using a collinear setup for the DOG. The configuration is similar to that for the conventional PG except the last quarter wave plate now consists of a quartz plate and a BBO crystal combination. The details of the setup will be reported elsewhere. The backing pressure is 20 torr, Figs. 4(a) and 4(b) show the harmonic spectra and the line profile, respectively. The main feature of the spectrum is the cutoff and plateau regions combine to form a smooth distribution covering more than 20 nm. The signal below 20 nm was truncated by the detector. Figure 4(c) shows that the Fourier transform-limited pulse has a marked reduction of the pre or post pulses and the spectrum is capable of supporting a 130 as duration. Oishi *et al.* demonstrated

high harmonic generation by a two-color gating with ~ 9 fs input pulses [26]. These results however only support structureless continua in the cutoff region (~ 3 nm, from 24 to 27 nm) leaving the plateau range with modulations in contrast to DOG.

In conclusion, we demonstrated an important step towards generating single isolated pulses using multiple-cycle driving lasers. By implementing the DOG technique, an extreme ultraviolet supercontinuum capable of supporting 130 as pulses was generated. The dependence of the harmonic spectra on the CE phase with 2π periodicity was discovered for the first time, which may lead to a new CE phasemeter with a large window suitable for long laser pulses. Because of the relaxation on the pump laser requirements, the DOG allows more researchers to enter the playground of attosecond science.

*chang@phys.ksu.edu.
[1] A. Scrinzi *et al.*, J. Phys. B **39**, R1 (2006).
[2] G. Sansone *et al.*, Science **314**, 443 (2006).
[3] M. Nisoli *et al.*, Opt. Lett. **22**, 522 (1997).
[4] M. Hentschel *et al.*, Nature (London) **414**, 509 (2001).
[5] P. B. Corkum *et al.*, Opt. Lett. **19**, 1870 (1994).
[6] V. Platonenko and V. Strelkov, J. Opt. Soc. Am. B **16**, 435 (1999).
[7] O. Tcherbakoff *et al.*, Phys. Rev. A **68**, 043804 (2003).
[8] B. Shan, S. Ghimire, and Z. Chang, J. Mod. Opt. **52**, 277 (2005).
[9] Z. Chang, Phys. Rev. A **70**, 043802 (2004).
[10] Z. Chang, Phys. Rev. A **71**, 023813 (2005).
[11] U. Andiel *et al.*, Europhys. Lett. **47**, 42 (1999).
[12] N. Dudovich *et al.*, Nature Phys. **2**, 781 (2006).
[13] J. Mauritsson *et al.*, Phys. Rev. Lett. **97**, 013001 (2006).
[14] M. Ammosov, N. Delone, and V. Krainov, Sov. Phys. JETP **64**, 1191 (1986).
[15] B. Shan, C. Wang, and Z. Chang, U.S. Patent No. 7 050 474, issued on May 23, 2006.
[16] H. Mashiko *et al.*, Appl. Phys. Lett. **90**, 161114 (2007).
[17] D. J. Jones *et al.*, Science **288**, 635 (2000).
[18] E. Moon *et al.*, Opt. Express **14**, 9758 (2006).
[19] C. Li, E. Moon, and Z. Chang, Opt. Lett. **31**, 3113 (2006).
[20] Z. Chang, Appl. Opt. **45**, 8350 (2006).
[21] C. Li *et al.*, Opt. Express **14**, 11 468 (2006).
[22] I. Sola *et al.*, Nature Phys. **2**, 319 (2006).
[23] P. B. Corkum, Phys. Rev. Lett. **71**, 1994 (1993).
[24] C. A. Haworth *et al.*, Nature Phys. **3**, 52 (2007).
[25] G. G. Paulus *et al.*, Phys. Rev. Lett. **91**, 253004 (2003).
[26] Y. Oishi *et al.*, Opt. Express **14**, 7230 (2006).